

A new GLM-based method for mapping tree cover continuous fields using regional MODIS reflectance data

Markus Schwarz, Niklaus E. Zimmermann*

Swiss Federal Research Institute WSL, Dept. of Landscape Research, Zuercherstrasse 111, 8903 Birmensdorf, Switzerland

Received 27 April 2004; received in revised form 5 November 2004; accepted 16 December 2004

Abstract

Knowledge about land cover and its change is an important input for the monitoring and modeling of ecological and environmental processes from the regional to the global scale. Considerable efforts have been made to develop global continuous fields for different land cover types at large spatial scales based on NOAA-AVHRR and TERRA-MODIS data and a range of techniques have been applied to depict the sub-pixel fraction of land cover types from these data. In this study, a new methodology is described for deriving and optimizing continuous fields of tree cover for complex topography at the regional scale of the European Alps using generalized linear models (GLM). MODIS data (MOD09) at a spatial resolution of 500 m were used to calibrate the models against regional training data of fractional tree cover. For evaluating the method we test the GLM model output to a regression tree model (using the same data structure). Further we test the resulting GLM-based tree cover continuous fields against two different, independent test data sets; one of which is spatially separated and the other is from within the calibration area. Finally, we compare the GLM model output with two available global data sets at spatial resolutions of 1 km and 3 km: (1) TERRA-MODIS Vegetation Continuous Fields product (MOD44), and (2) the NOAA-AVHRR vegetation continuous fields. Our GLM-based method results in high accuracy (MAE=9.1%) and low bias (−1.2%) across the combined evaluation and calibration area, and with small differences only between the calibration and the spatially separated evaluation area (1.3%). Compared to the regression tree model the results from the GLM model for all analyses are significantly better. Thus we conclude that generalized linear models are appropriate for deriving continuous fields of fractional tree cover for complex topography at the regional scale. GLMs can handle nonlinear relationships present in the training data set well, and the method is robust with respect to sample size and the number of months used for calibration. Regional calibrations of vegetation continuous fields may offer significantly improved predictions compared to globally calibrated models. Such regionally calibrated and optimized models may serve as valuable tools for regional monitoring of land cover pattern and its temporal change.

© 2005 Elsevier Inc. All rights reserved.

Keywords: European Alps; Fractional cover; Generalized linear models; GLM; Multi-temporal; MODIS; Tree cover continuous fields; Weighted kappa

1. Introduction

The environment of the European Alps with its characteristic complex topography and its fine-scale and often traditional land use regime is considerably exposed to both natural environmental threats and human impacts and exploitation (Tasser & Tappeiner, 2002). The combined pressure on the alpine environment arising from past

development, rapid land use change, tourism, and possible climate change (Barry, 1994; Grabherr et al., 1994; Theurillat & Guisan, 2001) is high when compared to other similar environments (Price & Haslett, 1995; Tasser & Tappeiner, 2002). According to the 1989 International Convention on the Protection of the Alps, mountain regeneration and sustainability are key issues. For sustainable use and management, and for large-area monitoring and modeling of these Alpine terrestrial habitats, consistent land cover information across national borders is indispensable (CIPRA, 2001). Additionally, such information is required for many aspects of earth sciences and analyses of global

* Corresponding author.

E-mail address: niklaus.zimmermann@wsl.ch (N.E. Zimmermann).

change, including resource management or biodiversity assessment (Townshend et al., 1994). The knowledge of spatial patterns and extent of terrestrial ecosystems is further important for the evaluation and management of carbon sinks and sources at national and continental levels, as land vegetation stores considerable amounts of comparably mobile carbon stocks (Cernusca et al., 1998). Tree cover mapping has particularly grown in importance as a result of the need to quantify the global woody biomass (Hansen et al., 2002). Finally, the knowledge of the distribution of tree cover is an important input to modeling of biogeochemical cycles and climate feedbacks (Sellers et al., 1997; Townshend et al., 1994). Thus, reliable land cover information and data sets are needed for a wide range of environmental monitoring applications. Previous studies have shown that remote sensing based data are appropriate tools to detect land cover change (Justice et al., 1998; Rogan et al., 2002).

Considerable efforts have recently resulted in the development of global and continental land cover data at small spatial scales based on the Advanced Very High Resolution Radiometer (NOAA-AVHRR) and the Moderate Resolution Imaging Spectroradiometer (TERRA-MODIS). Examples include: (1) the PELCOM land cover map (Mucher et al., 2000), (2) the UMD global land cover map (Hansen & Reed, 2000), (3) the IGBP-DIS continental and global land cover map (Belward et al., 1999; Loveland & Belward, 1997; Townshend et al., 1994), and (4) the MODIS MOD12 global land cover product (Friedl et al., 2002). The paradigm for describing the characteristics of the surface covered by these data sets is to classify each pixel into a land cover type based on a predefined classification scheme (DeFries & Townshend, 1994; DeFries et al., 1998). However, this approach has certain limitations (Aplin & Atkinson, 2001). In most cases, all degrees of mixing of pure land cover classes within a pixel can be found due to the continuum of variation found in the landscape (Foody & Hill, 1996) and the mixed nature of land cover at coarse (≈ 1 km) spatial resolution (Schowengerdt, 1996). This is especially true for complex landscapes of mountainous terrain and for small-scale structured landscape of traditional land use schemes with its typically small patches of human and natural disturbances. Hence, the discretization of land cover into a limited number of categories results in a loss of information (Ju et al., 2003). This loss of information can have significant impact on subsequent modeling as has been demonstrated, e.g., by Pierce and Running (1995). Alternatively, a number of techniques to depict the sub-pixel fraction of landscape components from the same remotely sensed data have been applied. In general, such techniques make use of high temporal resolution to overcome the restrictions of limited spatial resolution. Statistical approaches used so far (Fernandes et al., 2004; Hansen et al., 2002) are: (1) fuzzy membership functions (Foody, 1994; Foody & Cox, 1994), (2) artificial neural networks (Atkinson et al., 1997; Braswell et al., 2003), (3)

regression trees (DeFries et al., 1997), (4) decision trees (McIver & Friedl, 2002), and (5) linear mixture models (Adams et al., 1995). The resulting continuous field maps—containing the fraction of landscape components as a continuous variable—offer the advantage of summarizing the effects of spatial heterogeneity better than the discrete land cover maps based on the same data sources. As a result, such products have a higher potential to accurately monitor land cover change over time (Hansen et al., 2002).

Several attempts have recently been made to map fractional landscape components using moderate resolution imagery covering large areas. First investigations using AVHRR data made use of a linear mixture model to derive global continuous fields of multiple vegetation classes (DeFries et al., 1999). Recent efforts have shown that linear mixture models may not be suitable in cases when multiple scattering results in nonlinear mixing (Ju et al., 2003). In this context nonlinear decision rules may produce better results. Hansen et al. (2002) presented an improved technique to derive the fraction of tree cover per pixel using a combination of a regression tree algorithm and linear least-square models. The results showed that this method is an improvement over the linear-mixture model and it can better handle the nonlinear relationships present in a global sample of tree cover.

The goal of this paper is to present a new promising approach for fractional cover mapping of moderate resolution imagery based on generalized linear models (GLM) and using regional training data. GLMs are an extension of the linear (least-square regression) modeling that allows models to be fitted to data with errors following other than (only) Normal distributions, and for dependent variables following other than a Normal distribution, such as the Poisson, Binomial and Multinomial (McCullagh & Nelder, 1989). Ordinary least-squares regression assumes, e.g., that the model response varies continuously and that it is unbounded. GLMs of the binomial model family overcome this difficulty by linking the binary response to the explanatory covariates through the probability of either outcome, which varies continuously from 0 to 1 (Dobson, 2002). This approach is often referred to as logit regression. Other model families allow fitting response variables of different restricting characteristics (Poisson regression, etc.). Tree cover fractions have the same restrictions as binary dependent variables (upper and lower bounds); except they vary continuously between 0 and 1. Thus, GLMs of the binomial model family may be equally well applied to fractional cover data as can be applied to presence/absence data. While the GLM output of a binary response variable is interpreted as “probability to occur”, one can take the GLM output of a cover response at the original scale, which is cover fraction. GLMs are commonly used in environmental research (see Guisan & Zimmermann, 2000, for a review; Zimmermann & Kienast, 1999, for an application), though we found few examples with remote sensing data. One successful

application was carried out by [Morisette et al. \(1999\)](#) who explored the use of GLMs for enhancing standard methods of satellite-based land cover change detection.

In this study, we describe a methodology for deriving continuous fields of tree cover at the regional scale of the European Alps using generalized linear models and MODIS MOD09 data. Additionally, we present means to evaluate and optimize such models. In doing so, we explore the effect of the phenology (temporal range covered), the seasonal cloud cover, and the sample size upon the model quality. The procedure presented uses MODIS reflectance data (MOD09) at a spatial resolution of 500 m. The benefit of such a regionally optimized model is to establish accurate regional data sets to, e.g., (1) enable flexible change detection procedures, (2) account for regional characteristics (e.g., topography, phenology, vegetation), (3) support basin-scale hydrological or conservation studies, and (4) improve monitoring of regional-scale climate and land use effects upon tree vegetation. For purposes of evaluating the model approach we test the GLM model output to a regression tree model ([Breiman et al., 1984](#); [Chambers & Hastie, 1991](#)) using the same training and calibration data. Further we test our resulting continuous fields of tree classification against two available global data sets (1) the TERRA-MODIS Tree Cover Continuous Fields product (MOD44) based on regression trees at 500 m spatial resolution ([Hansen et al., 2002](#)), and (2) the NOAA-AVHRR Vegetation continuous fields using linear mixture models at a spatial resolution of 1000 m ([DeFries et al., 1999](#)).

2. Materials and methods

2.1. Study area

The Alps of Southern Central Europe extend over 1000 km from the Mediterranean coast of France and Northwestern Italy through Switzerland, Northern Italy, to Southern Germany, Austria, and Slovenia ([Fig. 1](#)). The highest peak is Mont Blanc at 4807 m. The Alps are characterized by an extraordinary biodiversity and a variety of landscapes, by geological, morphological and climatologic diversity, and by a long history of varying traditional land management. This results in highly complex structures and reflectance patterns. About one third of this mountainous landscape is covered by forest. Due to the large spatial extent and the wide altitudinal range a multitude of vegetation zones is present. In the Southern Alps the Mediterranean climate and warmer winter temperatures are responsible for the presence of evergreen broadleaf trees. The more northern areas of the Alps are affected by a temperate climate, with colder winters. Here, the forests are formed by broadleaf deciduous and coniferous (both evergreen and deciduous) trees, depending on elevation and specific site conditions. The core of the study area is in Switzerland, which shares all of the variety described above.

2.2. Calibration data

In order to calibrate our model of fractional tree cover, we used atmospherically corrected (the correction scheme

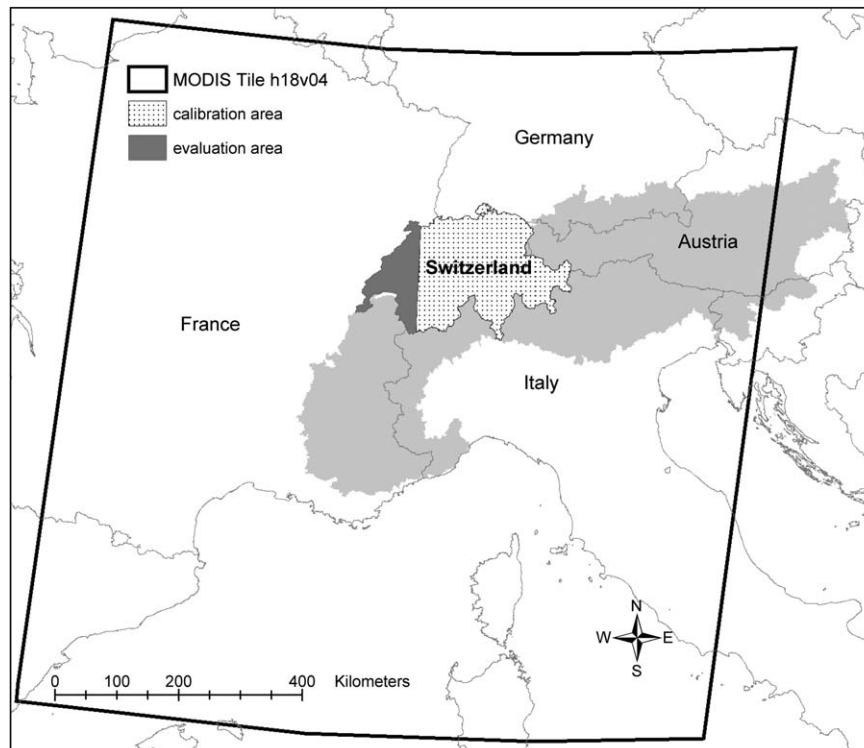


Fig. 1. Study area and the location of calibration and evaluation area (the grey shade shows the extent of the European Alps).

includes corrections for the effect of atmospheric gases, aerosol, and thin cirrus clouds (=6S code)) and georeferenced reflectance data from the Moderate Resolution Imaging Spectroradiometer (MODIS) on board the TERRA satellite at a spatial resolution of 500 m. The data set aggregated, as described below, represents the explanatory variables in our model. The surface reflectance product (MOD09) is a seven-band product computed from the MODIS Level 1B land bands 1, 2, 3, 4, 5, 6, and 7 (centered at 648 nm, 858 nm, 470 nm, 555 nm, 1240 nm, 1640 nm, and 2130 nm, respectively). Specifically, we used the MODIS level 3 surface reflectance product, MOD09_L3_V004, as an 8-day composite of the gridded, daily level 2 surface reflectance products, i.e., MOD09_L2G (Justice et al., 2002). We downloaded all tiles of h18v04 and h19v04, covering the entire extent of the European Alps, for the years 2001 and 2002 from the NASA's EOS data gateway.¹ The data were transformed to UTM coordinate system with WGS 1984 datum (Zone North 32). Further, the Normalized Difference Vegetation Index ($NDVI = (nir - red) / (nir + red)$) was calculated for each 8-day composite. To reduce the negative effect of cloud contamination we synthesized the 8-day composites to monthly images based on the maximum NDVI value per month (Holben, 1986). By doing this, each pixel acquires for each band the value of the 8-day composite map where the NDVI was highest, thereby reflecting optimal atmospheric conditions and advanced vegetation development. Based on these 12×8 data sets, one for each month for all seven 500 m bands and the NDVI, a series of new data sets were derived. First, a number of calibration data sets were generated for the year 2001 that contained the 12, 10, 8, 6, 4, and 2 months (thereafter called mx12, mx10, mx8, mx6, mx4, and mx2, respectively) with the highest NDVI values (and their corresponding reflectance) pixel by pixel. Selecting those months with highest NDVI was done to exclude the effect of varying seasonality across the study area, and to exclude noisy pixels independent of the month. From these data sets a number of metrics representing the seasonal and/or annual phenological characteristics of vegetation were derived according to DeFries et al. (1995, 1998) in order to maximize the discrimination among vegetation types. These metrics include the minimum, maximum, mean, range, and standard deviation per reflectance band and of the NDVI for each data set (mx2 to mx12). This results in ($8 \times 5 =$) 40 metrics per pixel for each calibration data set.² Next, a monthly set of calibration data was generated that only contained the

reflectance values of the highest NDVI value pixel by pixel. This was done to test the performance of the monthly model calibration throughout the year. Finally, from all calibration data sets (i.e., area-wide maps), sub-samples of 11,298 pixels within the boundary of the calibration area (Fig. 1) reflecting a regular lattice were re-sampled for model calibration. This represents 1/9th of the total surface within the calibration area. The remaining fraction (8/9th) was treated as an independent test data set to evaluate the model inside the calibration area (see Training and evaluation data sets). The western part of Switzerland outside of the calibration area was used to evaluate the model in a spatially separated area. To test the influence of sample size on the model quality, we derived additional sub-samples from the mx8 data set ranging from 111 up to 25,471 pixels, based on the same regular grid sampling by increasing the re-sampling distance in both x and y directions of the grids. All of the above described sampling schemes are based on MODIS data for 2001.

In order to test the potential of topography related variables for improving the model calibration, we used a digital terrain model from the Federal Office of Topography with 25 m grid size. From this terrain model, we derived elevation, slope and aspect, as well as potential global radiation. The latter variable was generated using the method of Kumar et al. (1997) for potential direct and diffuse radiation. For testing the effects of leaf phenology and meteorology upon the model quality, we generated a data set of the monthly average cloud cover fraction for Switzerland, using a set of 25 climate stations across Switzerland from daily data for the 2 years of 2001 and 2002. Based on these station data, we generated 24 monthly maps of average cloud cover fraction for the study area. Subsequently, we generated 24 monthly models (covering the years 2001 and 2002) using the seven bands and NDVI values as independent model parameters to further evaluate the effect of seasonality and the yearly differences on the resulting model quality.

2.3. Training and evaluation data sets

A training data set is required to calibrate the model and an evaluation data set is used to independently test the accuracy of the model. Both data sets represent response variables in our models. Here we used data from high-resolution satellite imagery for Switzerland. An existing Swiss forest map, based on 11 Landsat-5 TM images dating from 1990 to 1992, was used. It covers an area of nearly 45,000 km² and all images were collected between 14th July and 15th September. This high resolution forest map was re-projected to UTM coordinate system with the WGS 1984 datum (Zone North 32) used in the calibration. The forest map—available through the 100 m resolution GEOSTAT data package from the Swiss Federal Office of Statistics (Bundesamt fuer Statistik, 2001)—contains four different forest classes based on leaf morphology. The classes

¹ <http://www.redhook.gsfc.nasa.gov/~imswww/pub/imswelcome/index.html>.

² The advantage of annual metrics (including the “best months only”) versus the monthly metrics is that the former are not as sensitive to time of year or the seasonal cycle. By this, the model can reduce the influence of atmospheric contamination to a minimum (Hansen et al., 2002). This is a possibility to capture the optimal season and values per pixel \pm irrespective of the local phenological dynamics.

include: (1) broadleaf, (2) needleleaf, and mixed forests with predominantly (3) needleleaf, or (4) broadleaf trees. The average error of the map is 8.2%, which is comparable with the training data used by Hansen et al. (2002).

A linear regression model calibrated with tree cover information from forest inventory data (originating from 1992 to 1995) was used to convert the forest cover map into a spatial representation of tree cover per forested pixel. For areas not classified as forests, we used the “Swiss Areal Statistics 92/97”, available within the same GEOSTAT package to convert all pixels containing tree vegetation. To do so we applied the following rules: “Hedges” and “tree islands” were classified to 40% tree cover; fruit yards—30%; backyards of residential areas—15%; recreational areas (camping and golf yards, cemeteries, public parks)—15%. This approach is very similar to the methods used by DeFries et al. (1998) for converting different land cover types into tree cover fractions. The resulting tree cover values range between 0 and 95%. This 100 m grid was then aggregated to the resolution of the MODIS MOD09 (500 m) data, resulting in a data set with more than 150,000 pixels for calibration and testing. This data set was further split spatially into two parts: (1) the western part (8083 km²) serves as reference data to evaluate the model in a spatially separated region and (2) the eastern part (33,322 km²) serving partly as training data (1/9th of pixels for the standard model) to calibrate the model and partly as evaluation data (remaining pixels not used for calibration) to test the model accuracy. The resulting tree cover fractions are unevenly distributed (Fig. 2), following a Poisson like distribution. Specifically, low cover fractions are predominant. The averaged fractional cover in the evaluation area is slightly higher than in the calibration area (25% versus 23%) mostly due to a lower number of pixels with no or very low tree cover in the evaluation area (high-alpine

regions). The fact that this data set is 10 years old is not a severe limitation, since a federal law in Switzerland enforces the maintenance of the spatial extent of the forests, prohibiting the conversion of forests into other land cover types. Additionally, there is a strict fire suppression strategy, and a low intensity of timber harvesting (no large area clear-cuts). The only major causes of forest cover change are wind throw, and forest expansion due to land abandonment. Though, we expect that a model would be slightly better, if calibrated with more modern training data.

The final, regionally optimized model of tree cover fraction was evaluated at the native resolution of 500 m against the reference data. Additionally, we re-sampled the data set to a spatial resolution of (1) 1 km and (2) 3 km in order to compare our data set with available global data sets, one of which is only available at a resolution of 1 km. In order to reduce the effect of differing resolutions, we perform the comparison only at coarser resolutions.

2.4. Available global data sets

Up to the present, two global data sets containing the estimated fraction of tree cover are available, both from the University of Maryland. We do not intend to thoroughly test these data sets. Rather, we aim at comparing our results from a regionally optimized GLM model of tree cover fraction with the only available similar data sets for reference. Available global data sets are:

- (1) The NOAA-AVHRR vegetation continuous fields (called AVHRR-VCF, thereafter) product is based on data from the Advanced Very High Resolution Radiometer (NOAA-AVHRR). The data were acquired in 1992–1993 at a 1 km spatial resolution and processed under the guidance of IGBP (Eiden-

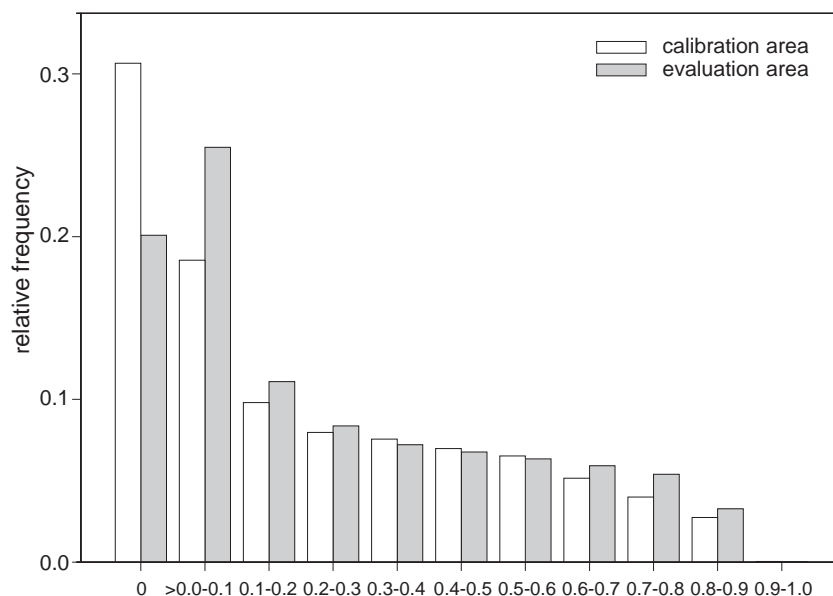


Fig. 2. The frequency distribution for the fractional tree cover based on the evaluation and calibration area, follows a Poisson distribution.

shink & Faundeen, 1994). The resulting continuous field products include (a) tree cover, (b) leaf type and (c) leaf longevity. The procedure for deriving the continuous fields of vegetation characteristics is fully explained in DeFries et al. (1999).³ The statistical method used is a linear mixture model. A set of 156 Landsat Multispectral Scanner data was used to train the linear models for vegetation characteristics, which allows estimation of the endmember values (DeFries et al., 1998). Constrained by the algorithm the fraction of tree cover ranges between 10% and 80% for each pixel. In order to enable a direct comparison with the other data sets used we re-projected the data set to the UTM coordinate system with WGS 1984 datum (Zone North 32) used in this study.

- (2) The TERRA-MODIS Vegetation Continuous Fields product MOD44 (called MODIS-VCF, thereafter) contains estimates of percent tree cover as developed from globally distributed, high-resolution training data. A regression tree model was used to link the MODIS MOD09 500 m reflectance data to the training data and phenological metrics. In order to span the tree cover values within each regression tree class, a linear least-squares regression model was calibrated within each class (Hansen et al., 2002). These linear models are then applied to all pixels that belong to the respective terminal nodes of the regression tree. By doing this, the predicted tree cover variable ranges continuously from 0 to 100%. The MOD44 product is assigned for estimating the fractional cover of: (a) life form (proportion of *woody vegetation*, *herbaceous vegetation*, or *bare ground*), (b) leaf type (proportion of *woody vegetation* that is needleleaf or broadleaf), (c) leaf longevity (proportion of *woody vegetation* that is evergreen or deciduous). The first release of the MODIS Vegetation Continuous Fields product (MOD44) is available for download since January 2003. This version contains the percent tree cover layer with other layers to follow in a later release. This product was generated from monthly composites of 500 m resolution MODIS data. The MOD09A1 surface reflectance 8-day composites were used as inputs to the 32-day composites. Compositing was based on the second darkest albedo to remove clouds and cloud shadow. All seven bands were used to derive metrics for the calculation of the percent tree cover with emphasis given to bands 1, 2, and 7 (Hansen et al., 2003). We re-projected this data set to UTM coordinate system with WGS 1984 datum (Zone North 32) used in this study.

Prior to comparison with the optimized GLM-based model, both data sets were re-sampled to a spatial resolution of (a) 1 km and (b) 3 km to enable a direct comparison. The re-sampling was intended to reduce spatial registration uncertainties and to minimize the point spread function effects (Huang et al., 2002).

2.5. Statistical model development

The basic idea of GLM is a generalization of the linear (=ordinary least-square regression) model described by McCullagh and Nelder (1989). In its simplest form, a linear model specifies the curvilinear relationship between a response variable Y , and a set of explanatory variables X_i , so that

$$Y = b_0 + b_1X_1 + b_2X_2 + \dots + b_kX_k + \varepsilon \quad (1)$$

where b_0 is the regression coefficient for the intercept and the b_k values are the regression coefficients for the explanatory variables 1 through k , computed between training data and a set of explanatory variables X_k (where X may be linear or of higher power), and ε is the error term.

For most data analysis problems, using least-square regressions of the linear model family is adequate to test or explain the importance of explanatory variables upon the observed dependent pattern. However, there are relationships that cannot adequately be summarized by ordinary least-square regressions, for two major reasons: (1) a bounded or non-normally distributed response variable, or (2) a binomial, multinomial, or ordinal multinomial (i.e., contain information on ranks only) instead of continuous response variables may exist (Lindsey, 1997; Venables & Ripley, 1999). GLM models can cope with a larger range of modeling problems by providing a number of model families (Binomial, Poisson, etc.), including the general least-square regression as a special case (Dobson, 2002; Green & Silverman, 1994; Guisan & Zimmermann, 2000).

We selected the binomial model family—also termed logit regression—to build our model in Splus (Insightful, 2001). This is the appropriate model family for a binomially distributed and bounded (between 0 and 100%) response variable. The converted and aggregated national tree cover map was used as the response variable. All basic statistics of the seven 500 m MODIS bands and the NDVI per pixel for the months used in the respective data sets (mx2 to mx12) were included as explanatory variables to calibrate the model. These included: (1) the minimum, (2) the maximum, (3) the range, (4) the average and (5) the standard deviation among all months used, resulting in a set of (5×8=) 40 explanatory variables. For the monthly data sets and models, we used the seven bands plus NDVI as predictive variables directly, since no summary statistics can be derived from a single band value per month. We built a full GLM model containing all possible explanatory variables. All powers up to the second order but no interactions were included in this model. A stepwise variable selection—allowing both back-

³ We downloaded the product from the *Global Land Cover Facility* of the University of Maryland, accessible through: <http://www.glcfc.umd.edu/data/>.

ward and forward selection—was applied thereafter, in order to optimize the final model. The stepwise model optimization is based on the Akaike's Information Criterion (AIC). We use the D^2 value (percent deviance explained) to evaluate the model fit, calculated as $(\text{Null.Deviance} - \text{Residual.Deviance}) / \text{Null.Deviance}$, where the Null.Deviance is the deviance of the model with the intercept only, and the Residual.Deviance is the deviance that remains unexplained after all final variables have been included. This is equivalent to the R^2 of a linear least-squares regression model.

For purpose of comparison we developed a regression tree model using the same calibration and training data. Tree based models provide a flexible alternative to linear regression problems. The models are fitted by binary recursive partitioning whereby a data set is successively split into increasingly homogeneous subsets until it is infeasible to continue (Venables & Ripley, 1999). We implemented the model in Splus (Insightful, 2001), and the algorithms used are described in Clark and Pregibon (1993). First, we fitted an initial tree with a minimum of three observations per terminal node. In order to reduce overfitting of such trees, we applied a repeated 10-fold crossvalidation procedure (Breiman et al., 1984). At each crossvalidation run, the training data is split randomly into 10 groups, where 90% of the data are used to optimize the node splits, while the left out 10% are used to test the error rate (deviance) at each node. Once each tenth is left out and used for validating once, the overall 10-fold crossvalidation output allows to determine the optimal number of tree nodes to prune the tree where deviance is minimized. We repeated this step nine times and determined the average optimal tree node for pruning, since each random split of one 10-fold crossvalidation results in a different optimal number of nodes. The final tree model used for comparison was subsequently pruned by the optimized node number beyond which the model could not improve further as seen from the repeated crossvalidation.

2.6. Model evaluation

The evaluation of the simulated continuous tree cover fraction against the reference data was performed using several statistical measures, namely: (1) the mean absolute error (MAE, see Eq. (2)), (2) the bias, (3) the correct classification rate (CCR), and (4) the weighted kappa (κ_w , see Eqs. (3)–(6)). Measures 3 and 4 were calculated based on a confusion matrix with the continuous dependent variables aggregated to strata of 25% width.

The calculation of the mean absolute error (MAE) of the simulated map compared to a reference map can be denoted as follows:

$$MAE = \frac{\sum_{i=1}^n |Z_{(xi)} - Z_{(Xi)}|}{n} \quad (2)$$

where, $Z(Xi)$ is the reference value at a given location i , $Z(xi)$ is the estimated value. MAE is an overall measure expressing the average of the pixel-by-pixel errors irrespective of their sign. The bias, on the other hand, is the mean of the error, thus emphasizing over- and underpredictions. The overall correct classification rate (CCR_o) of a target map compared to a reference map is the sum of the diagonal terms of the confusion matrix of i strata and is equivalent to the overall accuracy. CCR_i is the accuracy of a given stratum, and is equivalent to the producer's accuracy (diagonal term of the i th stratum divided by the sum of the i th column).

The kappa coefficient (κ), introduced by Cohen (1960), allows one to test if the agreement between a target map and a reference map is significantly better than by chance given the proportional numbers per stratum. The measure can be derived from the same $i \times i$ confusion matrix, with i nominal classes. The weighted kappa coefficient (κ_w) is an extended measure of the Cohen's kappa (Cohen, 1968; Fleiss et al., 1969). It can be used to weight the disagreements between simulated and reference map strata. κ_w is given by Eq. (3):

$$\kappa_w = \frac{P_{o(w)} - P_{e(w)}}{1 - P_{e(w)}} \quad (3)$$

using

$$P_{o(w)} = \sum_i^r \sum_j^r w_{ij} P_{ij} \quad (4)$$

and

$$P_{e(w)} = \sum_i^r \sum_j^r w_{ij} P_i P_j \quad (5)$$

where the weights w_{ij} are computed emphasizing the difference between the simulated (j) and the observed (i) fraction of tree cover per pixel (Eq. (6), where r stands for the value of the stratum with the highest cover fraction), thus weighting the degree of error in the confusion matrix and penalizing large disagreements (Cicchetti & Allison, 1971). This is a more appropriate measure for testing our predictions, since the degree of error can be addressed. A resulting value of 1 for κ_w indicates a perfect agreement, while a value of 0 describes agreement no better than by chance.

$$w_{ij} = 1 - \frac{|i - j|}{|r - 1|} \quad (6)$$

3. Results

We first describe the model calibration and the model evaluation of an optimized GLM model for predicting tree cover continuous fields. The optimized GLM-based model uses statistical derivatives of the seven monthly 500 m

MODIS reflectance bands (plus monthly NDVI) of the eight best months, pixel by pixel. A total of 11,298 training pixels located in eastern Switzerland were used to calibrate this model. Next, we describe results from a series of model optimization procedures, aimed at testing the impact of various factors that may have an effect on the model accuracy. Finally, we summarize the results of a comparison of our regionally calibrated model with available global data sets at spatial resolutions of 1 km and 3 km.

3.1. Model description

An example of the model, its accuracy, and a comparison with the training data is given in Fig. 3. The parameters of the model are listed in Appendix A. Tested in the spatially separated evaluation region the GLM-mx8 model over-

Table 1

Statistical performance measures for the model GLM-mx8 in the evaluation and in the calibration area (excluding all pixels used for model calibration)

	Evaluation area	Calibration area	Combined
Total area (km ²)	8083	29,620	41,405
Total forest (km ²)	2045	6808	9702
Pred. forest (km ²)	2134	6640	9808
Bias	4.4%	-2.5%	-1.2%
MAE	10.3%	9.0%	9.1%
CCR _o	0.699	0.723	0.718
κ_w	0.908	0.9154	0.914

estimates the tree cover by 4.4% (Table 1). The model results in a CCR_o of 0.70 and an MAE of 0.103 (an error of 10.3% tree cover on average), while κ_w is 0.91 (Table 1). The associated confusion matrix (Table 2) presents the accuracies of the individual cover strata. Highest accu-

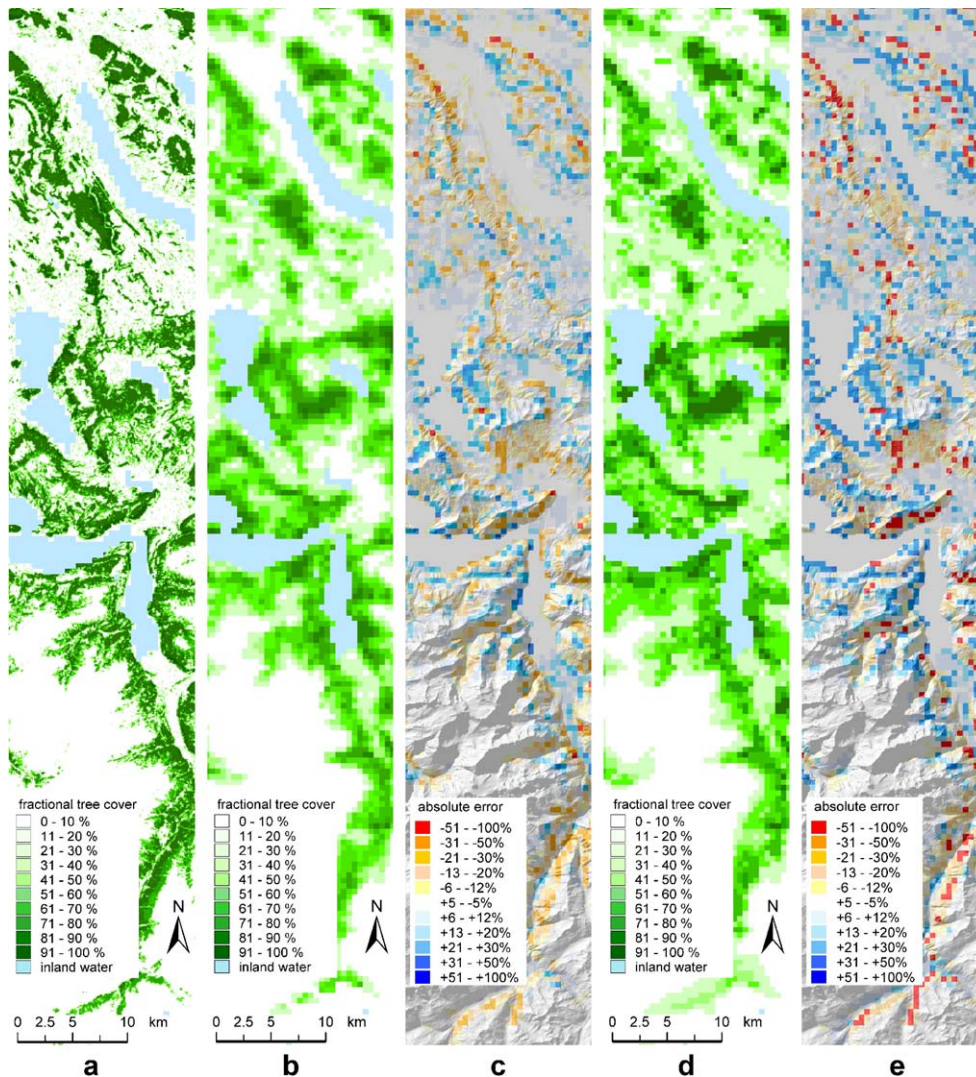


Fig. 3. Transect through Switzerland from North to South. (a) Fractional tree cover map based on the Swiss forest map and forest inventory data at a spatial resolution of 100 m used as training and evaluation data (©Bundesamt für Statistik, GEOSTAT, CH-2010 Neuchâtel), (b) the fractional tree cover prediction of the GLM-mx8 model (at a spatial resolution of 500 m), (c) absolute error of the GLM-mx8 model (calculated on the basis of a and b) draped over the shaded terrain model, (d) the fractional tree cover prediction of the regression tree model (at a spatial resolution of 500 m) and (e) absolute error of the regression tree model (calculated on the basis of a and d) draped over the shaded terrain model.

Table 2

Confusion matrix for the model GLM-mx8 reclassified to strata of 25% for the evaluation area

		Reference				Sum
		<25%	25–50%	50–75%	75–100%	
GLM-mx8	<25%	16,466	1383	280	27	18,156
	25–50%	2686	3023	1611	324	7644
	50–75%	323	1461	2877	1530	6191
	75–100%	1	9	90	243	343
	Sum	19,476	5876	4858	2124	32,334
CCR _{i/o}		84.5%	51.4%	59.2%	11.4%	69.9%

racies are obtained for the cover stratum 0–25% with an individual CCR_i of 0.85 followed by the stratum 50–75% with 0.59. For the other cover strata the individual CCR_i ranges between 0.51 (25–50%) and 0.11 (75%–100%). Within the calibration area the GLM-mx8 model underestimates the tree cover by 2.5% with an MAE of 0.09. The CCR_o reaches 0.72 and the κ_w 0.92. The associated confusion matrix (Table 3) gives details about the accuracies of the individual cover strata. Highest accuracies are again obtained for the cover stratum 0–25% with an individual CCR_i of 0.88 followed by the stratum 25–50% with 0.53. For the other cover strata the individual CCR_i ranges between 0.48 (50–75%) and 0.12 (75–100%). The overall accuracy of the model within the combined evaluation and calibration area is almost identical, since the model performs similarly within both regions (Table 1). The difference in model accuracy between evaluation and calibration area is only 0.013 (=1.3%) for MAE.

When assessing errors more in detail along the tree cover axis, we see only slight differences in the prediction accuracies between the calibration and evaluation areas (Fig. 4). The MAE of fractional cover of the GLM-based mx8 model tends to be stable below 60% tree cover, but then increases above this number. Also, the bias of the simulated tree cover is similar for both the evaluation and the calibration area (Fig. 5). Again both curves show the same characteristics and generally overpredict low fractional tree cover, and underpredict high observed cover fractions. However, the relative error is comparably high at low cover. Additionally, the low bias overall will not cancel out equally, if e.g., the model is applied to a sparsely vegetated area where the mx8 model tends to overpredict generally. The model can thus

be considered optimized for the forest cover of the European Alps.

3.2. Comparison with the regression tree model

When comparing the GLM model with the regression tree model, we were interested in testing the effect of sample size on model accuracy (MAE). By this, we aimed at testing if the GLM model is similar or better compared to the tree-based model, and if sample size has an influence on the order of the two models. Fig. 7 demonstrates that the achieved accuracies for the GLM model are better throughout compared to the regression tree model. The only exception is for very small sample sizes (<200), where the absolute difference between the two models slowly increase with the reduction of the sample size. Additionally, the differences in the accuracies tested in the calibration compared to the evaluation area are generally smaller for the GLM models.

3.3. Model optimization

Here, we present model optimization and sensitivity analyses. First, we were interested in testing the impact of the number of months required to accurately predict fractional tree cover. The results of the six derived data sets (mx12, mx10, mx8, mx6, mx4 and mx2) reveal that even with a minimum of two (best) months of MODIS MO09 data, we obtain satisfactory results (Fig. 6). Rather, using too many months (e.g., all 12 months)—instead of using the best *n* months only—reveals inferior results. Compared to the mx8 model, only the mx2 model differs significantly at the 0.99 confidence level. However, using

Table 3

Confusion matrix for the model GLM-mx8 reclassified to strata of 25% for the calibration area (excluding all pixels used for model calibration)

		Reference				Sum
		<25%	25–50%	50–75%	75–100%	
GLM-mx8	<25%	65,199	6373	1141	63	72776
	25–50%	7808	11,690	7097	1111	27706
	50–75%	796	3861	8049	4103	16,809
	75–100%	15	66	377	731	1189
	Sum	73,818	21,990	16,664	6008	118,480
CCR _{i/o}		88.3%	53.2%	48.3%	12.2%	72.3%

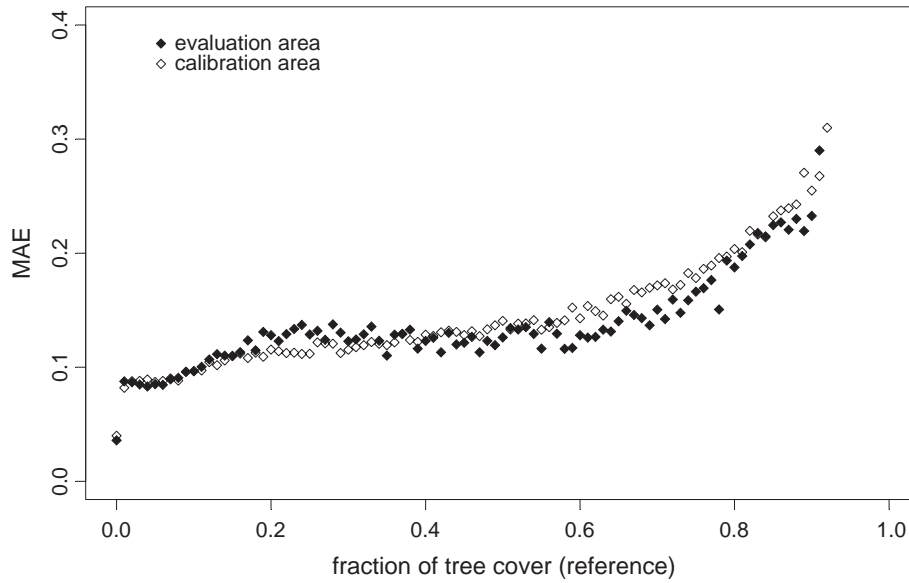


Fig. 4. Mean absolute error (MAE) ranges of fractional tree cover for the model GLM-mx8 in the evaluation and calibration area (excluding all pixels used for model calibration).

the best 2 months only, still results in a regional model that is superior to those obtained from global data sets (see Table 1 for comparison with MAE values). The model using data from the 4 (best) months (mx4) results in very comparable prediction accuracies with respect to MAE, and the model does not differ significantly from the mx8 model ($p=0.21$).

Next, we were interested in testing the effect of sample size on model accuracy (MAE). Fig. 7 shows that the accuracy decreased considerably when using less than 500 pixels for model calibration ($p<0.01$). However, sample sizes higher than 1000 pixels did not differ significantly from the standard mx8 model with respect to the resulting

MAE. The number of 1000 training pixels corresponds to $\approx 0.7\%$ of the training data set used for the mx8 model.

Analyzing the effect of adding topographic-variables reveals that the quality of the model can be improved significantly ($p<0.01$) by using elevation and slope as additional predictors. As a result, model quality (D^2) increases from 0.71 to 0.73, while the MAE of the calibrated model decreases slightly from 0.10 to 0.0975. The resulting κ_w increases to 0.92 compared to 0.91 without topographic variables, and the CCR_o increases from 0.70 to 0.72. The variables aspect and annual potential direct and diffuse radiation did not improve the model significantly ($p=0.67$).

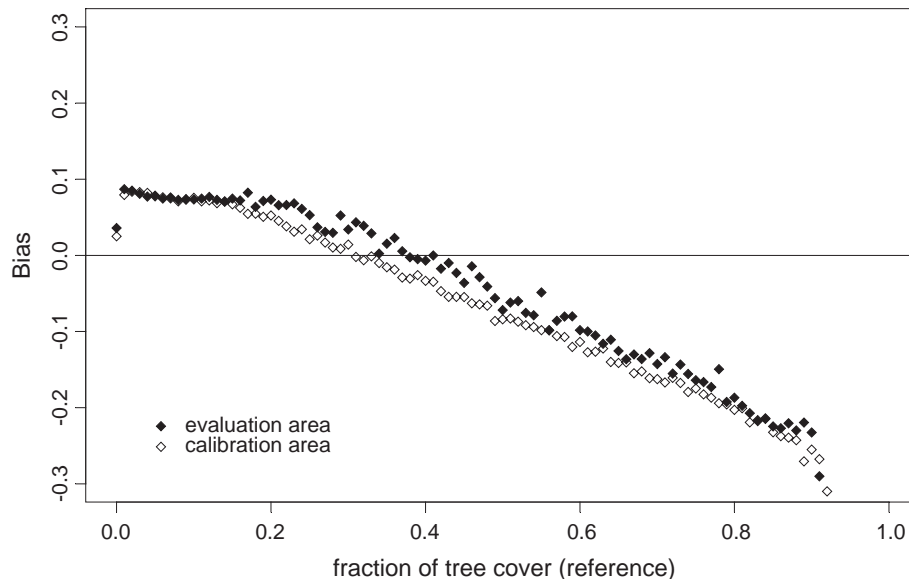


Fig. 5. Bias of the model GLM-mx8 for the evaluation and calibration area (excluding all pixels used for model calibration).

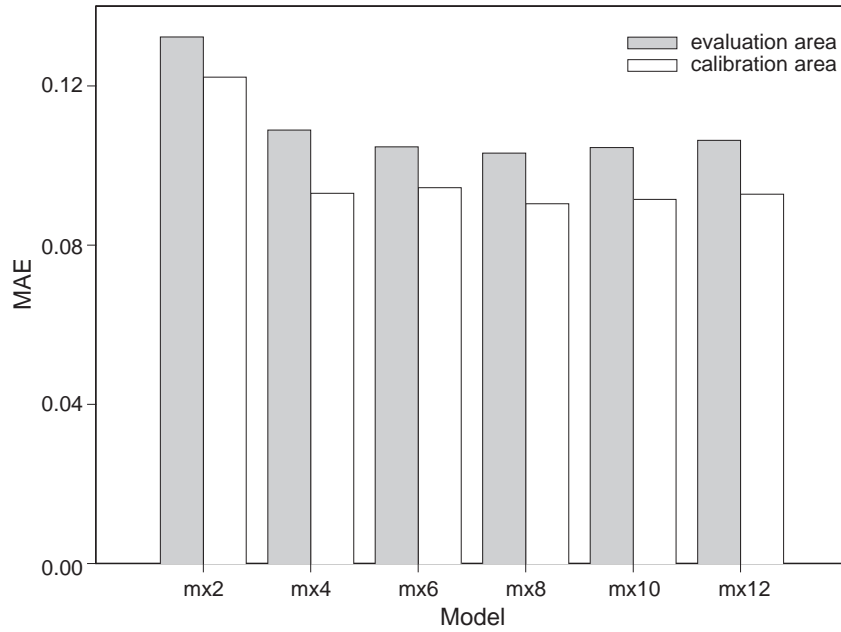


Fig. 6. The effect of the number of months used for model calibration on model accuracy (MAE).

Finally, we were interested in testing how the phenological state (seasonality) of vegetation affects the model quality. For this purpose, we tested the performance of single month models of the years 2001 and 2002. For evaluation, we compared the resulting D^2 values of the respective models, indicating the quality of the model fit with respect to the training data. Generally, the summer months produce models of higher quality than the winter months when snow cover is high, haze reduces the atmospheric transmittance, and foliage is absent. Addition-

ally, it becomes evident that for the year 2002, the monthly models did not reach the quality of the best months in 2001. We found that the monthly average of the fraction of clear-sky (inverse of percent cloud cover) correlates highly with the monthly D^2 sequence across the 2 years (Fig. 8). The resulting correlation between clear-sky fraction and model quality is $R=0.66$ when using all months, and $R=0.85$ when excluding the winter months (December to February) from the analysis when broadleaf trees have dropped their leaves.

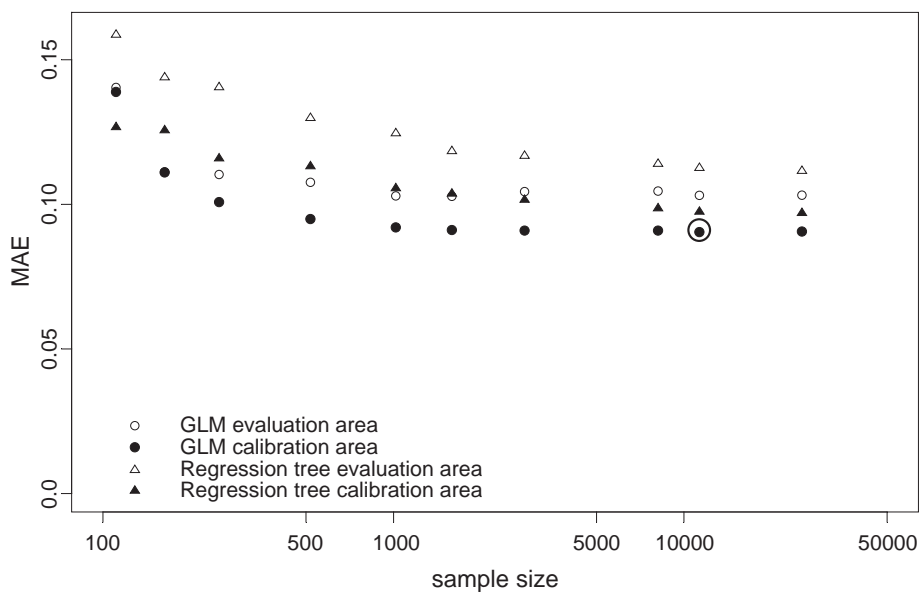


Fig. 7. Effect of sample size on model accuracy (MAE) tested on the independent evaluation data set (open symbols) and within the calibration area (closed symbols) for the GLM model (circles) and the regression tree model (triangles). The sample size for the standard model (mx8) calibrated in this analysis is indicated by a bold circle.

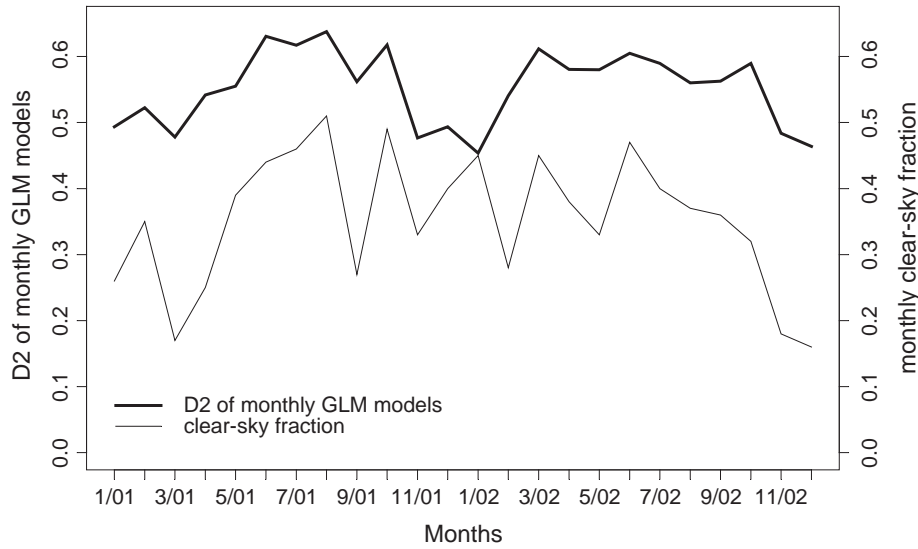


Fig. 8. Effect of seasonality (phenology) and average monthly clear-sky fraction on model fit (D^2). The average monthly fraction of clear-sky is calculated from 25 climate stations across Switzerland covering the whole area used for model calibration.

3.4. Comparison with other data sets

In addition to assessing model accuracy and optimization we were interested in comparing our standard GLM-mx8 model with similar maps, namely the global MODIS-VCF and AVHRR-VCF products. We were interested to see whether our regional model performs at least as well as other existing products. This was not done to test these other models, but instead to test the usability of the GLM-mx8 model. We evaluated the three products at the combined test site (evaluation and calibration area).

The derived accuracy measures are summarized in Table 4. At a spatial resolution of 1 km the GLM-mx8 model underestimates the tree cover by 1.5%. The model results in a CCR_o of 0.79, a MAE of 0.07, and a κ_w of 0.94. The MODIS-VCF data set overestimates the cover fraction by 72.2% and achieved a CCR_o of 0.52. The associated MAE is 0.19, while κ_w is 0.82. The AVHRR-VCF data set overestimates the fractional tree cover by 41.2% and achieved a CCR_o of 0.50. The MAE is 0.20, while κ_w is 0.81. At a spatial resolution of 3 km the GLM-mx8 model underestimates the tree cover by 1.9%. The

model results in a CCR_o of 0.87, an MAE of 0.04, and a κ_w of 0.96. The MODIS-VCF data set overestimates the cover fraction by 73.4% and achieved a CCR_o of 0.49. The associated MAE is 0.17, while κ_w is 0.82. The AVHRR-VCF data set overestimates the fractional tree cover by 41.9% and achieved a CCR_o of 0.55. The MAE is 0.15 and κ_w is 0.85.

4. Discussion

The results show that the GLM-mx8 model using 11,298 training pixels resulted in comparably high accuracies for both the evaluation and training areas. Figs. 4 and 5 show that the error of the GLM-mx8 model tends to be higher at higher observed cover fractions, with similar characteristics for both the evaluation and calibration areas. This may be the reason for the slightly higher MAE in the evaluation area, where more pixels with high fractional tree cover occur. The comparison between the GLM-mx8 model and the Swiss tree cover map shows a high spatial agreement (Fig. 3), even though the landscape- and forest-patterns are highly fragmented.

Table 4

Statistical performance measures for the model GLM-mx8, the global data sets MODIS-VCF and AVHRR-VCF at a spatial resolution of 1 km and 3 km for the entire test region (combined evaluation and calibration area)

	1 km resolution			3 km resolution		
	GLM-mx8	MODIS-VCF	AVHRR-VCF	GLM-mx8	MODIS-VCF	AVHRR-VCF
Total area (km ²)	41,396	41,396	41,396	41,508	41,508	41,508
Total tree cover (km ²)	9688	9688	9688	9612	9612	9612
Pred. tree cover (km ²)	9540	16,680	13,684	9432	16,668	13,644
Bias	-1.5%	72.2%	41.2%	-1.9%	73.4%	41.9%
MAE	0.066	0.194	0.196	0.039	0.174	0.152
CCR_o	0.786	0.521	0.501	0.869	0.486	0.549
κ_w	0.939	0.815	0.809	0.963	0.817	0.852

Further, the visual exploration of the error map reveals that fractional tree cover is generally overestimated in steep slopes of northern exposure, while likely to be underestimated in slopes of southern exposure (see northern parts of Fig. 3). This might be an effect of shadows on the model—an effect that is not directly captured by the parameters slope, aspect and elevation which we tested for model optimization. Also, the differences in the phenological development between north and south facing slopes might additionally affect the distribution of errors. Generally, the stationarity of the spatial error distribution and the same high accuracy for the evaluation and calibration area shows that the resulting model can be considered robust. Thus we conclude that GLM offer a simple, yet accurate method to calibrate vegetation continuous fields.

The additional models (mx12, mx10, mx8, mx6, mx4, mx2) reveal that the best results were achieved with the mx8 model. Fewer input-months resulted in a poorer quality of the resulting model. However, the decrease in accuracy becomes only statistically significant when using less than 4 months. The decreasing number of used months indicates a reduced representation of the phenological characteristics of a land pixel. On the other hand, the slightly reduced accuracies for the mx10 and mx12 models indicate that the presence of snow during the winter season has a negative effect upon model quality.

Surprisingly, comparably accurate models can be calibrated from relatively few training pixels (Fig. 7). This is very promising for using such regional models for rapid and accurate change detection. Such rapid detection is not easy to obtain from high resolution, precise regional data. A significant reduction in model accuracy

only occurred when we used less than 1000 training pixels, which corresponds to less than 0.7% of the total training data set used. This is consistent with experiences made in predictive habitat distribution modeling (see Guisan & Zimmermann, 2000 for a review), and it further indicates that the calibrated model can be considered robust.

The comparison with the regression tree models show that in our study the GLM models revealed constantly better accuracies. As mentioned in the results the differences between calibration area and evaluation area are constantly smaller for the GLM model. This indicates that the extrapolation of the GLM model to other alpine areas is more reliable from GLM models compared to tree based models. The reduced accuracy is most likely an effect of the discretization, where several differing band combinations result in the percent tree cover, where the GLM model predicts gradual changes. The method by Hansen et al. (2002) used to generate the MOD44 product overcomes this by applying a second (linear regression) model step to the pixels within each terminal node, thus spanning the clustered endmembers to a more gradual prediction.

The model calibration of individual months demonstrates two important characteristics: (1) due to phenological constraints, models of the summer period (April to October) proved to be superior, and (2) the individual monthly models correlated highly with the clear-sky fraction (Fig. 9), especially during the summer months. In the winter months, when the vegetation is not (well) developed and the surface is partially or entirely covered by snow, resulting model qualities are reduced. During the summer months, resulting model qualities are much

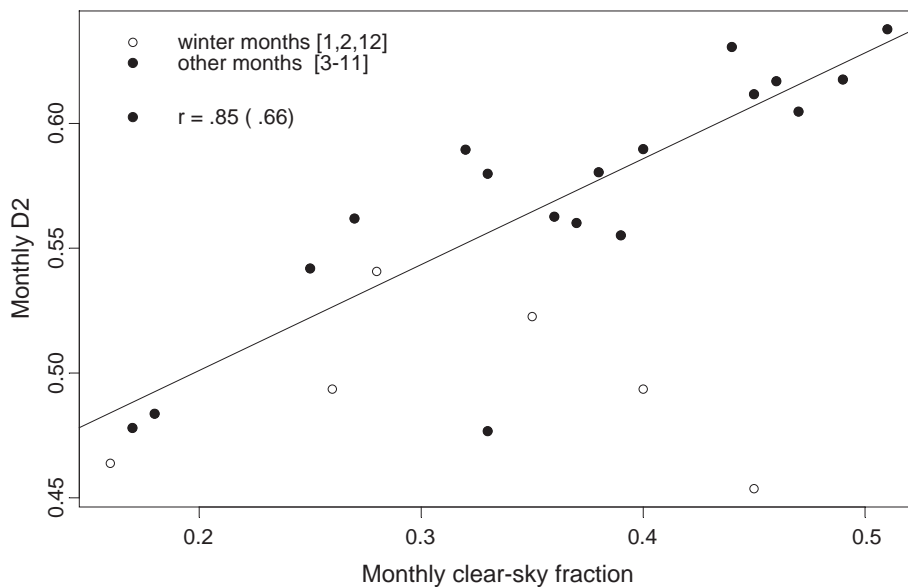


Fig. 9. Plot between the model fit (D^2) and average monthly clear-sky fraction. The correlation coefficient (r) between clear-sky fraction and model fit is $r=0.66$ for all months and $r=0.85$ (fit shown), when the winter months (December to February) are excluded from the analysis.

higher, and they correlate well with the clear-sky fraction—the inverse of the cloud cover fraction—for the calibration period. This indicates the importance of a high number of cloud free days per pixel to achieve a good model quality. If there are too many cloudy days the 8-day composites of the MOD09 products are not likely to map the true vegetation state. The D^2 of the best individual months model (August 2001) is 0.63. This is a very good model quality, when compared to the mx8 model with a D^2 value of 0.72. From this we learn that a comparably short period of cloud-free weeks can be sufficient to monitor the fractional tree cover efficiently. The fact that relative air humidity or vapor pressure deficits did not have a significant effect upon the model quality indicates efficient atmospheric correction. Most likely, the model could be further improved by rigorously using the quality flags on cloud and atmospheric conditions for masking optimal pixels for model calibration. This seems especially important when calibrating large areas, where atmospheric conditions vary considerably across such spatial scales.

The MODIS-VCF and AVHRR-VCF classifications generally overestimate tree fractional cover in the complex topography of the European Alps. For the study area, the accuracies revealed for both spatial resolutions analyzed significantly lower accuracies compared to the regionally calibrated GLM model. The possible sources for these differences are: (1) the training (response) data used, (2) spatial uncertainties, (3) the algorithm used, or (4) used explanatory variables (calibration). We do not further evaluate possible sources, since we did not aim at testing these models, nor comparing the algorithms. However, from our optimization exercise we learned that the quality of the explanatory variables (here MOD09) and the quality of the response variables used play a crucial role for the resulting model accuracy. This may be especially true for temporally composited layers.

5. Conclusion

As several prior efforts have shown (DeFries et al., 1999; Hansen et al., 2002, 2003), vegetation continuous fields provide a useful and promising alternative to the traditional discrete classification approaches. The reduction in thematic resolution and in the spatial distribution of information is minimal at this low spatial resolution compared to other data sets and models at higher spatial resolution (e.g., Landsat TM). As a consequence, this method offers a sound approach to detect land cover change. Since a high temporal resolution increases model accuracy (Fig. 6), TERRA-MODIS or NOAA-AVHRR offers an optimal source for rapid change detection. Generalized linear models are easy to calibrate and showed high model accuracy. The statistics applied is

well suited for deriving fractional tree cover at the scale of the European Alps, revealing better results than from regression tree models. GLMs are well able to handle nonlinear relationships present in the training data set. The method seems to be robust since an equally high accuracy was achieved for both the evaluation and calibration areas. Thus, this model can be applied to a spatially separated area in the context of the European Alps. Our analysis of the model showed that even with a small number of training pixels (≈ 1000) good results were achieved and that topographic variables can improve the quality of the model as well. Furthermore, we conclude that the method is robust with respect to the number of months used for calibration. However, and this is likely true for other statistical methods as well, careful attention should be given to periods with low clear-sky fractions when composited data sets are used. Also, the winter months do not provide significant information for mapping fractional tree cover.

In contrast to the investigated global data sets, which use worldwide training data for model calibration (MODIS-VCF and AVHRR-VCF), and hence are designed for continental to global applications, we optimized the model at the regional scale of the European Alps with training data characteristic solely of the investigated area. The differences between data sets are the result of different factors like training data, predictor layers, spatial uncertainties and algorithm. For sustainable use, optimal management and for large scale monitoring and modeling of these Alpine terrestrial habitats, it is critical to first obtain homogeneous, consistent and as far as possible, highly accurate information across national borders. While both global data sets offer similar quality and ideal tools for continental to global applications, it seems obvious that for certain regional applications where high accuracies or rapid change detection may be required, a regionally calibrated model will be a more appropriate instrument. In accordance with Hansen et al. (2002, 2003), we conclude that the improved spatial characteristics of MODIS data result in more accurate predictions compared to AVHRR-VCF based maps, not only at the global, but also at the regional scale.

Acknowledgments

We would like to thank Lukas Mathys, Otto Wildi, and Felix Kienast for fruitful discussions. Comments of Lukas Mathys and two anonymous reviewers helped us to improve the manuscript considerably. Portions of this research were funded by the 5th and 6th Framework Programme of the European Union (Contract Numbers EVK2-CT-2002-00136 and GOCE-CT-2003-505376), the Swiss Agency for Environment, Forest and Landscape (Project MfM-U), and by the Swiss Federal Research Institute WSL (Project Number 3.01.1313).

Appendix A

The GLM-mx8 model was calibrated with the constant term = -5.411e+00. The additional model parameters are listed below. Note that these are GLM output parameters.

	NDVI	B1	B2	B3	B4	B5	B6	B7
Ave	-7.453e-03	8.631e-03	-2.408e-04	3.408e-03	-1.606e-02	-3.985e-04	4.668e-03	-4.482e-04
Ave ²	1.755e-05	1.523e-07	-3.457e-07	-1.737e-07	9.174e-07	5.648e-07	-1.341e-06	1.970e-08
Max	4.553e-02	-9.566e-04	-4.154e-04	-1.393e-05	1.881e-03	1.288e-04	-5.022e-04	3.353e-04
Max ²	-3.738e-06	-4.460e-08	6.410e-08	-6.910e-08	2.390e-08	-4.430e-08	7.210e-08	-1.119e-07
Min	-4.173e-02	-	-	-	-	-	-	-
Min ²	2.868e-07	-	-	-	-	-	-	-
Range	-4.391e-02	-	-	-	-	-	-	-
Range ²	-2.044e-06	-	-	-	-	-	-	-
Std	1.531e-02	-	-	-	-	-	-	-
Std ²	8.238e-06	-	-	-	-	-	-	-

In order to predict fractional tree cover based on the calibrated parameters, the resulting function has to be converted to the original scale using the inverse of the logit-link function [i.e., $\text{Cover fraction} = \exp(f(x)) / (1 + \exp(f(x)))$].

References

- Adams, J. B., Sabol, D. E., Kapos, V., Almeida, R., Roberts, D. A., Smith, M. O., et al. (1995). Classification of multispectral images based on fractions of endmembers: Application to land-cover change in the Brazilian Amazon. *Remote Sensing of Environment*, 52, 137–154.
- Aplin, P., & Atkinson, P. M. (2001). Sub-pixel land cover mapping for per-field classification. *International Journal of Remote Sensing*, 22, 2853–2858.
- Atkinson, P. M., Cutler, M. E. J., & Lewis, H. (1997). Mapping sub-pixel proportional land cover with AVHRR imagery. *International Journal of Remote Sensing*, 18, 917–935.
- Barry, R. G. (1994). Past and potential future changes in mountain environments: A review. In M. Beniston (Ed.), *Mountain Environments in Changing Climates* (pp. 3–33). London: Routledge.
- Belward, A. S., Estes, J. E., & Kline, K. D. (1999). The IGBP-DIS global 1-km land-cover dataset DISCover: A project overview. *Photogrammetric Engineering and Remote Sensing*, 65, 1013–1020.
- Braswell, B. H., Hagen, S. C., Frolking, S. E., & Salas, W. A. (2003). A multivariable approach for mapping sub-pixel land cover distributions using MISR and MODIS: Application in the Brazilian Amazon region. *Remote Sensing of Environment*, 87, 243–256.
- Breiman, L., Friedman, J. H., Olshen, R. A., & Stone, C. J. (1984). *Classification and Regression Trees*. New York: Chapman & Hall.
- Bundesamt fuer Statistik (2001). *GEOSTAT Benutzerhanduch*. Neuenburg, Switzerland: Author. 458 pp.
- Cernusca, A., Tappeiner, U., Bahn, M., Bayfield, N., Chemini, C., Fillat, F., Graber, W., Rosset, M., Siegwolf, R., & Tenhunen, J. (1998). ECOMONT: An European approach for assessing ecological effects of land-use changes in mountain landscapes. In U. Tappeiner, F. V. Ruffini, & M. Fumai (Eds.), *Hydrology, Water Resources and Ecology of Mountain Areas* (pp. 163–167). Bozen, Italy: European Academy Bozen/Bolzano.
- Chambers, J. M., & Hastie, T. J. (1991). *Statistical Models in S*. New York, USA: Springer Verlag.
- Cicchetti, D. V., & Allison, T. (1971). A new procedure for assessing reliability of scoring EEG sleep recordings. *American Journal of E.E.G. Technology*, 41, 101–109.
- CIPRA (2001). 2. Alpenreport. Daten, Fakten, Probleme, Lösungsansätze. Verlag Paul Haupt, Bern, Stuttgart, Wien. 434 pp.
- Clark, L. A., & Pregibon, D. (1993). Tree-based models. In J. M. Chambers, & T. J. Hastie (Eds.), *Statistical Models in S* (pp. 377–419). London: Chapman & Hall.
- Cohen, J. (1960). A coefficient of agreement for nominal scales. *Educational and Psychological Measurement*, 20, 37–46.
- Cohen, J. (1968). Weighted kappa: Nominal scale agreement with provision for scaled disagreement or partial credit. *Psychological Bulletin*, 70, 213–220.
- DeFries, R., Hansen, M., Steininger, M., Dubayah, R., Sohlberg, R., & Townshend, J. (1997). Subpixel forest cover in central Africa from multisensor, multitemporal data. *Remote Sensing of Environment*, 60, 228–246.
- DeFries, R. S., Hansen, M., Townshend, J. (1995). Global discrimination of land cover types from metrics derived from AVHRR Pathfinder data. *Remote Sensing of Environment*, 54, 209–222.
- DeFries, R. S., Hansen, M., Townshend, J. R. G., & Sohlberg, R. (1998). Global land cover classifications at 8 km spatial resolution: The use of training data derived from Landsat Imagery in decision tree classifiers. *International Journal of Remote Sensing*, 19, 3141–3168.
- DeFries, R. S., & Townshend, J. R. G. (1994). NDVI-derived land cover classification at global scales. *International Journal of Remote Sensing*, 15, 3567–3586.
- DeFries, R. S., Townshend, J. R. G., & Hansen, M. C. (1999). Continuous fields of vegetation characteristics at the global scale at 1-km resolution. *Journal of Geophysical Research, D: Atmospheres*, 104, 911–916, 925.
- Dobson, A. J. (2002). *An Introduction to Generalized Linear Models*. Boca Raton: Chapman & Hall/CRC. 225 pp.
- Eidenshink, J. C., & Faundeen, J. L. (1994). The 1 km AVHRR global land data set: First stages in implementation. *International Journal of Remote Sensing*, 15, 3443–3462.
- Fernandes, R., Fraser, R., Latifovic, R., Cihlara, J., Beaubien, J., & Du, Y. (2004). Approaches to fractional land cover and continuous field mapping: A comparative assessment over the BOREAS study region. *Remote Sensing of Environment*, 89, 234–251.
- Fleiss, J. L., Cohen, J., & Everitt, B. S. (1969). Large sample standard errors of kappa and weighted kappa. *Psychological Bulletin*, 72, 323–332.
- Foody, G. M. (1994). Ordinal-level classification of sub-pixel tropical forest cover. *Photogrammetric Engineering and Remote Sensing*, 60, 61–65.
- Foody, G. M., & Cox, D. P. (1994). Sub-pixel land-cover composition estimation using a linear mixture model and fuzzy membership functions. *International Journal of Remote Sensing*, 15, 619–631.
- Foody, G. M., & Hill, R. A. (1996). Classification of tropical forest classes from Landsat TM data. *International Journal of Remote Sensing*, 17, 2353–2367.

- Friedl, M. A., McIver, D. K., Hodges, J. C. F., Zhang, X. Y., Muchoney, D., Strahler, A. H., et al. (2002). Global land cover mapping from MODIS: Algorithms and early results. *Remote Sensing of Environment*, 83, 287–302.
- Grabherr, G., Gottfried, M., & Pauli, H. (1994). Climate effects on mountain plants. *Nature*, 369, 448–449.
- Green, P. J., & Silverman, B. W. (1994). *Nonparametric Regression and Generalized Linear Models, a Roughness Penalty Approach*. London: Chapman and Hall. 182 pp.
- Guisan, A., & Zimmermann, N. E. (2000). Predictive habitat distribution models in ecology. *Ecological Modelling*, 135(2–3), 147–186.
- Hansen, M. C., DeFries, R. S., Townshend, J. R. G., Carroll, M., Dimiceli, C., & Sohlberg, R. A. (2003). Global percent tree cover at a spatial resolution of 500 meters: First results of the MODIS vegetation continuous fields algorithm. *Earth Interactions*, 7(10), 1–15.
- Hansen, M. C., DeFries, R. S., Townshend, J. R. G., Sohlberg, R., Dimiceli, C., & Carroll, M. (2002). Towards an operational MODIS continuous field of percent tree cover algorithm: Examples using AVHRR and MODIS data. *Remote Sensing of Environment*, 83, 303–319.
- Hansen, M. C., & Reed, B. (2000). A comparison of the IGBP DISCover and University of Maryland 1 km global landcover products. *International Journal of Remote Sensing*, 21, 1365–1373.
- Holben, B. N. (1986). Characteristics of maximum-value composite images from temporal AVHRR data. *International Journal of Remote Sensing*, 7, 1417–1434.
- Huang, C. Q., Townshend, J. R. G., Liang, S. L., Kalluri, S. N. V., & DeFries, R. S. (2002). Impact of sensor's point spread function on land cover characterization: Assessment and deconvolution. *Remote Sensing of Environment*, 80, 203–212.
- Insightful (2001). *S-Plus 6 for Windows: User's Guide*. Seattle: Insightful. 688 pp.
- Ju, J., Kolaczyk, E. D., & Gopal, S. (2003). Gaussian mixture discriminant analysis and sub-pixel land cover characterization in remote sensing. *Remote Sensing of Environment*, 84, 550–560.
- Justice, C. O., Townshend, J. R. G., Vermote, E. F., Masuoka, E., Wolfe, R. E., Saleous, N., et al. (2002). An overview of MODIS Land data processing and product status. *Remote Sensing of Environment*, 83, 3–15.
- Justice, C. O., Vermote, E., Townshend, J. R. G., Defries, R., Roy, D. P., Hall, D. K., et al. (1998). The Moderate Resolution Imaging Spectroradiometer (MODIS): Land remote sensing for global change research. *IEEE Transactions on Geoscience and Remote Sensing*, 36(4), 1228–1249.
- Kumar, L., Skidmore, A. K., & Knowles, E. (1997). Modelling topographic variation in solar radiation in a GIS environment. *International Journal of Geographical Information Science*, 11(5), 475–497.
- Lindsey, J. K. (1997). *Applying Generalized Linear Models*. New York: Springer-Verlag. 256 pp.
- Loveland, T. R., & Belward, A. S. (1997). The International Geosphere Biosphere Programme Data and Information System global land cover dataset (DISCover). *Acta Astronautica*, 41, 681–689.
- McCullagh, P., & Nelder, J. A. (1989). *Generalized Linear Models*. London: Chapman and Hall. 511 pp.
- McIver, D. K., & Friedl, M. A. (2002). Using prior probabilities in decision-tree classification of remotely sensed data. *Remote Sensing of Environment*, 81, 253–261.
- Morissette, J. T., Khorram, S., & Mace, T. (1999). Land-cover change detection enhanced with generalized linear models. *International Journal of Remote Sensing*, 20, 2703–2721.
- Mucher, C. A., Steinnocher, K. T., Kressler, F. P., & Heunks, C. (2000). Land cover characterization and change detection for environmental monitoring of PAN-Europe. *International Journal of Remote Sensing*, 21, 1159–1181.
- Pierce, L. L., & Running, S. W. (1995). The effects of aggregating subgrid land-surface variation on large-scale estimates of net primary production. *Landscape Ecology*, 10, 239–253.
- Price, M. F., & Haslett, J. R. (1995). In N. J. R. Allan (Ed.), *Climate Change and Mountain Ecosystems, Mountains at Risk: Current Issues in Environmental Studies* (pp. 73–97). New Delhi: Manohar.
- Rogan, J., Franklin, J., & Roberts, D. A. (2002). A comparison of methods for monitoring multitemporal vegetation change using Thematic Mapper imagery. *Remote Sensing of Environment*, 80(1), 143–156.
- Schowengerdt, R. A. (1996). On the estimation of spatial-spectral mixing with classifier likelihood functions. *Pattern Recognition Letters*, 17, 1379–1387.
- Sellers, P. J., Dickinson, R. E., Randall, D. A., Betts, A. K., Hall, F. G., Berry, J. A., Collatz, G. J., Denning, A. S., Mooney, H. A., Nobre, C. A., Sato, N., Field, C. B., & HendersonSellers, A. (1997). Modelling the exchanges of energy, water and carbon between continents and the atmosphere. *Science*, 275, 502–509.
- Tasser, E., & Tappeiner, U. (2002). The impact of land-use changes in time and space on vegetation distribution in mountain areas. *Applied Vegetation Science*, 5, 173–184.
- Theurillat, J.-P., & Guisan, A. (2001). Impact of climate change on vegetation in the European Alps: A review. *Climatic Change*, 50, 77–109.
- Townshend, J. R. G., Justice, C. O., Skole, D., Malingreau, J. P., Cihlar, J., -P., Teillet, P., et al. (1994). The 1 km resolution global dataset: Needs of the International Geosphere Biosphere Program. *International Journal of Remote Sensing*, 15, 3417–3442.
- Venables, W. N., & Ripley, B. D. (1999). *Modern Applied Statistics with S-PLUS* (3rd edition). New York: Springer. 501 pp.
- Zimmermann, N. E., & Kienast, F. (1999). Predictive mapping of alpine grasslands in Switzerland: Species versus community approach. *Journal of Vegetation Science*, 10(4), 469–482.